ARCHIVES OF ELECTRICAL ENGINEERING VOL. 67(4), pp. 739–753 (2018)

DOI 10.24425/aee.2018.124737

Minimum dispersion coefficient criteria based positioning algorithm for BDS

LINA WANG, LINLIN LI

School of Computer and Communication Engineering
University of Science and Technology Beijing (USTB)
100083, Beijing, P. R. China
e-mail: wln_ustb@126.com

(Received: 08.03.2018, revised: 18.07.2018)

Abstract: The BeiDou navigation satellite system (BDS) is one of the four global navigation satellite systems. More attention has been paid to the positioning algorithm of the BDS. Based on the study on the Kalman filter (KF) algorithm, this paper proposed a novel algorithm for the BDS, named as the minimum dispersion coefficient criteria Kalman filter (MDCCKF) positioning algorithm. The MDCCKF algorithm adopts minimum dispersion coefficient criteria (MDCC) to remove the influence of noise with an alpha-stable distribution (ASD) model which can describe non-Gaussian noise effectively, especially for the pulse noise in positioning. By minimizing the dispersion coefficient of the positioning error, the MDCCKF assures positioning accuracy under both Gaussian and non-Gaussian environment. Compared with the original KF algorithm, it is shown that the MDCCKF algorithm has higher positioning accuracy and robustness. The MDCCKF algorithm provides insightful results for potential future research.

Key words: alpha-stable distribution, BeiDou satellites, Kalman filter, minimum dispersion coefficient criteria, non-Gaussian noise, positioning algorithm

1. Introduction

The Beidou navigation satellite system (BDS) is the third mature global navigation satellite system (GNSS) after GPS and GLONASS systems, established and managed by China independently [1]. The capable navigation service area has covered the Asia-Pacific region, and will have global coverage by 2020 [2]. In recent years, the BDS has received more and more attention, and developed rapidly in military and civilian areas [1–3]. As a result of a wide range of application areas, more and more applications need higher accuracy to satisfy the positioning requirements, and many scholars have deeply researched various optimization of positioning algorithms [4–14]. The positioning accuracy of navigation satellite systems will be subject to many factors, including multipath effects, tropospheric effects, ionospheric effects, which make the noise have a strong pulse. Under such conditions, the noise does not meet Gaussian distribution, and the probability density function often has a serious drag tail [15].

www.czasopisma.pan.pl PAN POLSKA AKADEMIA NAUK www.journals.pan.pl

If the noise distribution is described simply by the Gaussian model, its characteristics will not be fully characterized. And the accuracy of the positioning algorithm will be affected.

The most commonly used positioning algorithm for the BDS is Kalman filtering (KF) algorithm based on minimum mean squared error (MMSE) criteria, which is suitable for multi-variable systems, time-varying systems and non-stationary stochastic processes [16, 17]. However, when the noise does not obey the Gaussian distribution, there does not exist the second-order statistics of the received data [18]. In that case, the performance of the traditional KF algorithm will seriously degrade or even fail. Therefore, an appropriate model is needed to describe non-Gaussian noise effectively. John P. Nolan proposed the alpha-stable distribution (ASD) upon researching Central Limit Theorem, while the Gaussian model is one of the special cases in the ASD [19]. And then, Nikias et al. found that the noise with a strong pulse including multipath effects, atmospheric noise and so on can be effectively described by the ASD model [20]. Consequently, the ASD is adopted to describe the noise environment of the BDS in this paper.

To eliminate the adverse influences of true noise, many scholars have studied the state estimation. D. Magill proposed the multiple-model filter which forms the noise as a weighted sum of Gaussians [21]. Since the number of modes increases exponentially with the number of filters, the problem of multiple-model filters is the higher computational complexity. Reza Izanloo *et al*. proposed a Kalman filter algorithm based on the maximum correntropy criterion [22]. The maximum correntropy criterion can handle the non-Gaussian noise effectively by processing higher order statistics of noise [22]. But for the low-order noise, its performance will be very poor. The Monte Carlo (MC) sampling method is often used to deal with the non-Gaussian noise. The MC's key is that it can filter signals on the basis of maintaining the mean and variance characteristics of non-Gaussian noise [23]. As a non-linear method, the MC method filtering through the collection of sampling points, will increase the system complexity, and can not be well applied to real-time positioning system.

The existing research results can not be well used for the BDS. Therefore a more generally applicable positioning algorithm is proposed in this paper. To improve the positioning accuracy under both the Gaussian and non-Gaussian noises modeled by the ASD, the minimum dispersion coefficient criteria Kalman filter (MDCCKF) positioning algorithm for the BDS is proposed. To make up for the deficiencies of the MMSE criterion, this paper will combine more applicable minimum dispersion coefficient criteria (MDCC) to minimize non-Gaussian errors. Numerical results have shown that the MDCCKF algorithm could greatly improve the BDS's accuracy under the non-Gaussian environment. And what's more, it can be adaptive with the pulse intensity of noise, thereby improving the robustness of the positioning algorithm.

This paper is organized as follows: the KF based positioning algorithm for the BDS is introduced in Section 2, the proposed MDCCKF algorithm is described in Section 3 and the performance evaluation is presented in Section 4. Finally, the conclusions are drawn in Section 5.

2. KF based positioning algorithm in the BDS

In the BDS, the mobile station receives the observed data of BeiDou satellites, including an ephemeris and pseudo-range, and then calculates its position according to the received data [24].

www.czasopisma.pan.pl PAN POLSKA AKADEMIA NAUK www.journals.pan.pl

The receiver's coordinates will be solved according to the observation equation, including the pseudo-range observation equation and Doppler observation equation.

Let (x_u, y_u, z_u) denote the coordinate of a mobile station, (x_s^i, y_s^i, z_s^i) denote the coordinate of the i-th visual satellite where $i > 0$. Then, the geometric distance from the mobile receiver to the i-th satellite is:

$$R_u^i = \sqrt{\left(x_u - x_s^i\right)^2 + \left(y_u - y_s^i\right)^2 + \left(z_u - z_s^i\right)^2} . \tag{1}$$

The pseudo-range observation equation is as follows:

$$\rho_u^i = R_u^i + ct_u + I_i + T_i + \varepsilon_i . \tag{2}$$

Here, ρ_u^i is the pseudo-range from the i-th satellite to the mobile receiver; c is the speed of light; t_u represents the time-offset estimation of the mobile receiver; I_i and T_i denote the pseudo-range changes caused by ionosphere and troposphere, respectively; ε_i is the sum of errors which is not directly reflected in the equation.

Since that I_i and T_i can be got by the BDS's ephemeris, there are four unknowns in (2): the coordinates of mobile receiver (x_u, y_u, z_u) and time-offset estimation t_u. Therefore, more than four satellites are needed to calculate the coordinate of the receiver by minimizing ε_i.

Set the priori value of receiver coordinates and time-offset as $(\hat{x}_u, \hat{y}_u, \hat{z}_u)$, $\hat{t}_u$ respectively. By the Taylor expansion equation of (2), ε_i is obtained as (3).

$$\varepsilon_i = \frac{\hat{x}_u - x_s^i}{\hat{R}_u^i}\delta x_u + \frac{\hat{y}_u - y_s^i}{\hat{R}_u^i}\delta y_u + \frac{\hat{z}_u - z_s^i}{\hat{R}_u^i}\delta z_u + c\delta t_u - \rho_u^i - I_i - T_i - R_u^i - c\hat{t}_u . \tag{3}$$

Here, $\hat{R}_u^i = \sqrt{(\hat{x}_u - x_s^i)^2 + (\hat{y}_u - y_s^i)^2 + (\hat{z}_u - z_s^i)^2}$ represents the geometric distance from the priori coordinate value of the mobile receiver to the coordinate of the i-th satellite.

But when the receiver is moving, it is also necessary to establish the Doppler observation equation [25].

$$f_{di} = -\frac{f_0}{c}\frac{(\boldsymbol{P}_s^i - \boldsymbol{P}_u)\cdot(\boldsymbol{V}_s^i - \boldsymbol{V}_u)}{\boldsymbol{P}_s^i - \boldsymbol{P}_u} + ct_u' + \varepsilon_{di} \tag{4}$$

where f_0 is the carrier frequency; $\boldsymbol{P}_s^i = (x_s^i, y_s^i, z_s^i)$ is the satellite position vector; $\boldsymbol{P}_u = (x_u, y_u, z_u)$ is the positioning terminal position vector; $\boldsymbol{V}_s^i = (v_{sx}^i, v_{sy}^i, v_{sz}^i)$ is the satellite velocity vector; $\boldsymbol{V}_u = (v_{ux}, v_{uy}, v_{uz})$ is the positioning terminal velocity vector; ε_{di} is the sum of errors not directly reflected in the equation.

Similarly, let the priori value of receiver velocity and time-offset be $(\hat{v}_{ux}, \hat{v}_{uy}, \hat{v}_{uz})$, $\hat{t}_u'$ respectively. Through the Taylor expansion equation of (4), ε_{di} is obtained as (5).

$$\begin{aligned}\varepsilon_{di} = {} & \frac{f_0}{c}\left(\frac{v_{sx}^i - \hat{v}_{ux}}{\hat{R}_v^i} + \frac{x_s^i - \hat{x}_u}{(\hat{R}_v^i)^3}\right)\delta x_u + \frac{f_0}{c}\left(\frac{v_{sy}^i - \hat{v}_{uy}}{\hat{R}_v^i} + \frac{y_s^i - \hat{y}_u}{(\hat{R}_v^i)^3}\right)\delta y_u \\ & + \frac{f_0}{c}\left(\frac{v_{sz}^i - \hat{v}_{uz}}{\hat{R}_v^i} + \frac{z_s^i - \hat{z}_u}{(\hat{R}_v^i)^3}\right)\delta z_u + \frac{f_0}{c}\left(\frac{x_s^i - \hat{x}_u}{\hat{R}_v^i}\right)\delta v_x + \frac{f_0}{c}\left(\frac{y_s^i - \hat{y}_u}{\hat{R}_v^i}\right)\delta v_y \\ & + \frac{f_0}{c}\left(\frac{z_s^i - \hat{z}_u}{\hat{R}_v^i}\right)\delta v_z + c\delta t_u' - \left(f_{di} - \hat{f}_{di} - c\hat{t}_u'\right)\end{aligned} . \tag{5}$$

www.czasopisma.pan.pl PAN POLSKA AKADEMIA NAUK www.journals.pan.pl

Here, $\hat{R}_v^i = \sqrt{(\hat{v}_{ux} - v_{sx}^i)^2 + (\hat{v}_{uy} - v_{sy}^i)^2 + (\hat{v}_{uz} - v_{sz}^i)^2}$ represents the geometric distance from the priori velocity of the mobile receiver to the velocity of the i-th satellite.

To achieve higher positioning accuracy, ε_i and ε_{di} are needed to be minimized appropriately and the KF algorithm based on the MMSE criterion is commonly used [26]. The KF algorithm can merely deal with second-order statistics of noise, belonging to the range of second-order statistical theory [21, 27].

The dynamic equations of the KF algorithm can be expressed as

$$\boldsymbol{X}(k+1) = \boldsymbol{\Phi}\boldsymbol{X}(k) + \boldsymbol{\Gamma}\boldsymbol{W}(k), \tag{6}$$

$$\boldsymbol{Y}(k) = \boldsymbol{H}\,\boldsymbol{X}(k) + \boldsymbol{U}(k), \tag{7}$$

where $k \in N^+$ indicates the value of time; the state value of the time k is $\boldsymbol{X}(k) \in R^n$; $\boldsymbol{W}(k) \in R^r$ is the input state noise; $\boldsymbol{\Phi}$ represents the state transition matrix; $\boldsymbol{\Gamma}$ denotes the driving noise matrix; $\boldsymbol{Y}(k) \in R^n$ is the observed value of the time k; $\boldsymbol{U}(k) \in R^m$ is the reserved noise; $\boldsymbol{H}$ represents the prediction matrix.

After initializing the KF's state value, the input state parameter matrix $\boldsymbol{X}$ is defined as (8).

$$\boldsymbol{X} = \left[x_u, y_u, z_u, t_u, v_{ux}, v_{uy}, v_{uz}, t_u'\right]^T. \tag{8}$$

In general, $\boldsymbol{W}(k)$ and $\boldsymbol{U}(k)$ are Gaussian white noises with mean zero. The variance matrices of $\boldsymbol{W}(k)$ and $\boldsymbol{U}(k)$ are $\boldsymbol{Q}$ and $\boldsymbol{R}$ respectively.

$$\begin{cases} E\left[\boldsymbol{W}(k)\right] = 0 \\ E\left[\boldsymbol{U}(k)\right] = 0 \\ E\left[\boldsymbol{W}(k)\boldsymbol{W}^T(l)\right] = \boldsymbol{Q}\delta_{kl} \\ E\left[\boldsymbol{U}(k)\boldsymbol{U}^T(l)\right] = \boldsymbol{R}\delta_{kl} \end{cases}, \tag{9}$$

where δ_{kl} is the Kronecker delta function.

The key problem of the KF algorithm is that the value of estimate state $\hat{X}(l|k)$ with minimum variance can be solved based on the observed signal $[Y(1), Y(2), \cdots, Y(n)]$ where n is the number of observations. Under the MMSE criterion, the performance index function can be described as (10).

$$J = E\left(\left(\boldsymbol{X}(l) - \hat{\boldsymbol{X}}(l|k)\right)^T \left(\boldsymbol{X}(l) - \hat{\boldsymbol{X}}(l|k)\right)\right). \tag{10}$$

Through minimizing performance index (10) and combining with lemma 1, the recursion relation can be obtained [28].

Lemma 1 (projective theorem) [29]: Suppose that $\boldsymbol{x} \in R^n$, $y(1), y(2), \cdots, y(k) \in R^m$, and the second-order statistics of them exist. Then, it holds that

$$\begin{aligned} \text{proj}\left[\boldsymbol{x}|y(1), y(2), \cdots, y(k)\right] &= \text{proj}\left[\boldsymbol{x}|y(1), y(2), \cdots, y(k-1)\right] + \\ &+E\left[\boldsymbol{x}\boldsymbol{\varepsilon}^T(k)\right]\left\{E\left[\boldsymbol{\varepsilon}(k)\boldsymbol{\varepsilon}^T(k)\right]\right\}^{-1}\boldsymbol{\varepsilon}(k) \end{aligned}, \tag{11}$$

where $\boldsymbol{\varepsilon}(k) = \boldsymbol{y}(k) - \hat{\boldsymbol{y}}(k|k-1)$.

www.czasopisma.pan.pl PAN POLSKA AKADEMIA NAUK www.journals.pan.pl

The projective theorem is the starting point for the KF algorithm. The derivation process based on the projective theorem is introduced in detail in [28]. Due to space limitation, this section just lists the derivation of conclusions as follows:

The step state transition equation is

$$\hat{\boldsymbol{X}}(k+1|k) = \boldsymbol{\Phi}\hat{\boldsymbol{X}}(k|k), \tag{12}$$

where $\boldsymbol{\Phi}$ denotes a state transition matrix of time $k+1$.

The state update equation is

$$\hat{\boldsymbol{X}}(k+1|k+1) = \hat{\boldsymbol{X}}(k+1|k) + \boldsymbol{K}(k+1)\varepsilon(k+1). \tag{13}$$

Here,

$$\boldsymbol{K}(k+1) = \boldsymbol{P}(k+1|k)\boldsymbol{H}^T \left[\boldsymbol{H}\,\boldsymbol{P}(k+1|k)\boldsymbol{H}^T + \boldsymbol{R}\right]^{-1}, \tag{14}$$

$$\boldsymbol{\varepsilon}(k+1) = \boldsymbol{Y}(k+1) - \boldsymbol{H}\hat{\boldsymbol{X}}(k+1|k), \tag{15}$$

where $\boldsymbol{K}(k+1)$ is the filter gain matrix; $\boldsymbol{H}$ indicates a prediction matrix of time $k+1$; $\boldsymbol{\varepsilon}(k+1)$ indicates the residual value between the estimated value and the observed value.

The step prediction covariance matrix is:

$$\boldsymbol{P}(k+1|k) = \boldsymbol{\Phi}\boldsymbol{P}(k|k)\boldsymbol{\Phi}^T + \boldsymbol{\Gamma}\boldsymbol{Q}\boldsymbol{\Gamma}^T. \tag{16}$$

The covariance matrix update equation is:

$$\boldsymbol{P}(k+1|k+1) = [\boldsymbol{I}_n - \boldsymbol{K}(k+1)\boldsymbol{H}]\,\boldsymbol{P}(k+1|k). \tag{17}$$

Here,

$$E\left[X(0|0)\right] = \hat{X}(0|0) = \mu_0, \tag{18}$$

$$E\left(\left(X(0|0) - \mu_0\right)^T \left(X(0|0) - \mu_0\right)\right) = P(0|0) = P_0. \tag{19}$$

The traditional KF algorithm is not required to calculate the nominal trajectory formerly, but it cannot handle high-order and low-order noise effectively due to the linearization [27]. It can be seen from the performance index function of (10) that the KF algorithm processes the positioning results based on the second-order statistics theory. Therefore, the KF algorithm is optimal in the case of Gaussian noises. But for other noise distributions, an appropriate noise model is needed. In this paper, we use the MDCC to reduce the effects of real positioning noises.

3. Minimum dispersion coefficient criteria based positioning algorithm

Since the KF algorithm just uses the second-order signal information, it is not optimal in non-Gaussian noise environments [22]. In order to resolve the defect of the original algorithm, this paper proposes the minimum dispersion coefficient criteria based Kalman filter (MDCCKF) positioning algorithm.

www.czasopisma.pan.pl PAN POLSKA AKADEMIA NAUK www.journals.pan.pl

To reasonably denote the positioning noise, the ASD model developed by John P. Nolan is introduced. Its characteristic function can be expressed as (20) [23].

$$\phi(t) = \exp\Big\{j\delta t - \gamma|t|^{\alpha}\left[1 + j\beta\,\mathrm{sign}(t)\,\omega(t,\alpha)\right]\Big\}, \tag{20}$$

where j indicates the unreal figure.

$$\omega(t,\alpha) = \begin{cases} \tan\left(\dfrac{\pi\alpha}{2}\right), & \alpha \neq 1 \\ \dfrac{2}{\pi}\log|t|, & \alpha = 1 \end{cases}, \qquad \mathrm{sign}(t) = \begin{cases} 1, & t > 0 \\ 0, & t = 0 \\ -1, & t < 0 \end{cases}, \tag{21}$$

$$0 < \alpha \leq 2; \quad -1 \leq \beta \leq 1; \quad \gamma > 0; \quad -\infty < \delta < +\infty, \tag{22}$$

where α is the pulse index, which can determine the degree of random process pulse; β is the symmetric coefficient; γ is the dispersion coefficient that is similar to the variance of Gaussian distribution; δ is the position parameter to describe the mean or median of the ASD. As can be seen, the ASD is decided by these four parameters, but for ease of calculation, the $S\alpha S$ distribution as definition 1 is adopted in this paper.

Definition 1 (distribution) [20]: If $\beta \equiv 0$, then such multivariate stable distributions are symmetric and called symmetric α stable ($S\alpha S$).

Non-Gaussian noises, which are caused by multipath effects, atmospheric noise and so on, exist in the observed signal commonly while state noise of the BDS has small number of strong pulses. Therefore, to be more suitable for the practical application scene and reduce the complexity of the positioning algorithm, the ASD's $S\alpha S$ can be used as the observation noise model in this paper, while the state noise remains the Gaussian distribution. The spatial model described in formulas (6) and (7) should be amended as:

$$\boldsymbol{X}(k+1) = \Phi\boldsymbol{X}(k) + \boldsymbol{\Gamma}\boldsymbol{W}(k), \tag{23}$$

$$\boldsymbol{Y}_{nG}(k) = \boldsymbol{H}\boldsymbol{X}(k) + \boldsymbol{U}_{\mathrm{ASD}}(k), \tag{24}$$

where $\boldsymbol{Y}_{nG}(k)$ is the observed value including the ASD noise; $\boldsymbol{U}_{\mathrm{ASD}}(k)$ is the observed noise obeying the ASD model.

The paper addresses the dispersion coefficient defined as definition 2 to handle the noise.

Definition 2 (dispersion coefficient) [20]: let b be $S\alpha S$ random variables with $1 < \alpha \leq 2$, zero location parameters. Then the dispersion coefficient of b is

$$\gamma_b = [b,b]_{\alpha} = \|b\|_{\alpha}^{\alpha}. \tag{25}$$

So, the dispersion coefficients of the observation error is given in (26).

$$\gamma_{oe} = \|\boldsymbol{U}_{\mathrm{ASD}}(k)\|_{\alpha}^{\alpha} = \|\boldsymbol{Y}_{nG}(k) - \boldsymbol{H}\boldsymbol{X}(k)\|_{\alpha}^{\alpha}. \tag{26}$$

Minimizing the dispersion coefficient of the observed error makes it equal to the solution of $\|\boldsymbol{Y}_{nG}(k) - \boldsymbol{H}\boldsymbol{X}(k)\|_{\alpha}$. Moreover, the α-norm is proportional to p-order statistics [19].

Lemma 2 (lower-order theory) [20]: let d be an ASD variable. Then,

$$\begin{cases} E(|d|^p) < \infty, & 0 \leq p < \alpha \\ E(|d|^p) = \infty, & p \geq \alpha \end{cases}. \tag{27}$$

www.czasopisma.pan.pl PAN POLSKA AKADEMIA NAUK www.journals.pan.pl

According to the lower-order theory of lemma 2, when $1 < p < \alpha \leq 2$, the p-order statistics of observation error exists, signifying $E\left(|\boldsymbol{Y}_{nG}(k) - \boldsymbol{H}\boldsymbol{X}(k)|^p\right) < \infty$. Therefore, the definition of the performance index function is (28).

$$J_{MDCC} = E\left(\left|\boldsymbol{Y}_{nG}(k) - \boldsymbol{A}\boldsymbol{H}\hat{\boldsymbol{X}}(k)\right|^p\right) < \infty \tag{28}$$

where $\boldsymbol{A} = \mathrm{diag}(a_1, a_2, \cdots, a_n)$ is defined as a coefficient matrix.

It is necessary to minimize the error by solving the appropriate element value of $\boldsymbol{A}$. Therefore, minimizing the performance function, the derivative can be find out as (29).

$$\begin{aligned}\frac{\partial J_{MDCC}}{\partial a_h} &= -p\left|y_h(k) - a_h\boldsymbol{H}_{h*}\hat{\boldsymbol{X}}(k)\right|^{p-1}\left(\boldsymbol{H}_{h*}\hat{\boldsymbol{X}}(k)\right)^T \mathrm{sign}\left(y_h(k) - a_h\boldsymbol{H}_{h*}\hat{\boldsymbol{X}}(k)\right) \\ &= -p\left|y_h(k) - a_h\boldsymbol{H}_{h*}\hat{\boldsymbol{X}}(k)\right|^{p-1}\boldsymbol{H}_{h*}\hat{\boldsymbol{X}}(k)\mathrm{sign}\left(y_h(k) - a_h\boldsymbol{H}_{h*}\hat{\boldsymbol{X}}(k)\right)\end{aligned}, \tag{29}$$

where $y_h(k)$ is the element of observation vector $\boldsymbol{Y}_{nG}(k)$; a_h is the diagonal element of matrix $\boldsymbol{A}$; $\boldsymbol{H}_{h*}$ is the line vector of prediction matrix $\boldsymbol{H}$. The coefficient a_h has only the iterative solution given in (30).

$$\begin{aligned}a_h(g+1) = a_h(g) - p\left|y_h(k) - a_h(g)\boldsymbol{H}_{h*}\hat{\boldsymbol{X}}(k)\right|^{p-1}\boldsymbol{H}_{h*}\hat{\boldsymbol{X}}(k) \\ \mathrm{sign}\left(y_h(k) - a_h(g)\boldsymbol{H}_{h*}\hat{\boldsymbol{X}}(k)\right)\end{aligned}. \tag{30}$$

Here, $a_h(g)$ is the value of a_h at the g-th iteration, $\forall g \in N^+$.

Define the residual amount $r_g = y_h(k) - a_h(g)\boldsymbol{H}_{h*}\hat{\boldsymbol{X}}(k)$, (30) can be simplified as (31).

$$a_h(g+1) = a_h(g) - p\left|r_g\right|^{p-1}\boldsymbol{H}_{h*}\hat{\boldsymbol{X}}(k)\mathrm{sign}\left(r_g\right), \tag{31}$$

where $\hat{\boldsymbol{X}}(k)$ is determined by state Equation (23).

When $\left(\left|r_{g+1}\right| - \left|r_g\right|\right) / \left|r_g\right| < \varepsilon$, a_h stops iterating. Then all the a_h make up the matrix $\boldsymbol{A} = \mathrm{diag}(a_1, a_2, \cdots, a_n)$.

Then the coefficient matrix $\boldsymbol{A}$ can be solved and the ASD noise was minimized.

The observed equation removing the ASD noise can be got as (32).

$$\boldsymbol{Y}(k) = \boldsymbol{A}\,\boldsymbol{H}\,\boldsymbol{X}(k) + \boldsymbol{U}(k). \tag{32}$$

(23) and (32) are the spatial models to describe the dynamic system. Then, the MDCCKF algorithm will be derived according to projective theorem [29].

The step state transition equation is:

$$\hat{\boldsymbol{X}}(k+1|k) = \boldsymbol{\Phi}\hat{\boldsymbol{X}}(k|k). \tag{33}$$

The state update equation is:

$$\hat{\boldsymbol{X}}(k+1|k+1) = \hat{\boldsymbol{X}}(k+1|k) + \boldsymbol{K}(k+1)\,\boldsymbol{\varepsilon}(k+1). \tag{34}$$

Here,

$$\boldsymbol{K}(k+1) = \boldsymbol{P}(k+1|k)(\boldsymbol{A}\boldsymbol{H})^T\left[\boldsymbol{A}\boldsymbol{H}\boldsymbol{P}(k+1|k)(\boldsymbol{A}\boldsymbol{H})^T + \boldsymbol{R}\right]^{-1}, \tag{35}$$

www.czasopisma.pan.pl PAN POLSKA AKADEMIA NAUK www.journals.pan.pl

$$\boldsymbol{\varepsilon}(k+1) = \boldsymbol{Y}(k+1) - \boldsymbol{A}\,\boldsymbol{H}\,\hat{\boldsymbol{X}}(k+1|k). \tag{36}$$

The step prediction covariance matrix is:

$$\boldsymbol{P}(k+1|k) = \boldsymbol{\Phi}\boldsymbol{P}(k|k)\boldsymbol{\Phi}^{T} + \boldsymbol{\Gamma}\boldsymbol{Q}\boldsymbol{\Gamma}^{T}. \tag{37}$$

The covariance matrix update equation is:

$$\boldsymbol{P}(k+1|k+1) = [\boldsymbol{I}_n - \boldsymbol{K}(k+1)\,\boldsymbol{A}\,\boldsymbol{H}]\,\boldsymbol{P}(k+1|k). \tag{38}$$

Then, the coordinate and velocity can be calculated according to (34)~(38).
The flowchart of the MDCCKF based positioning algorithm is shown in Fig. 1.

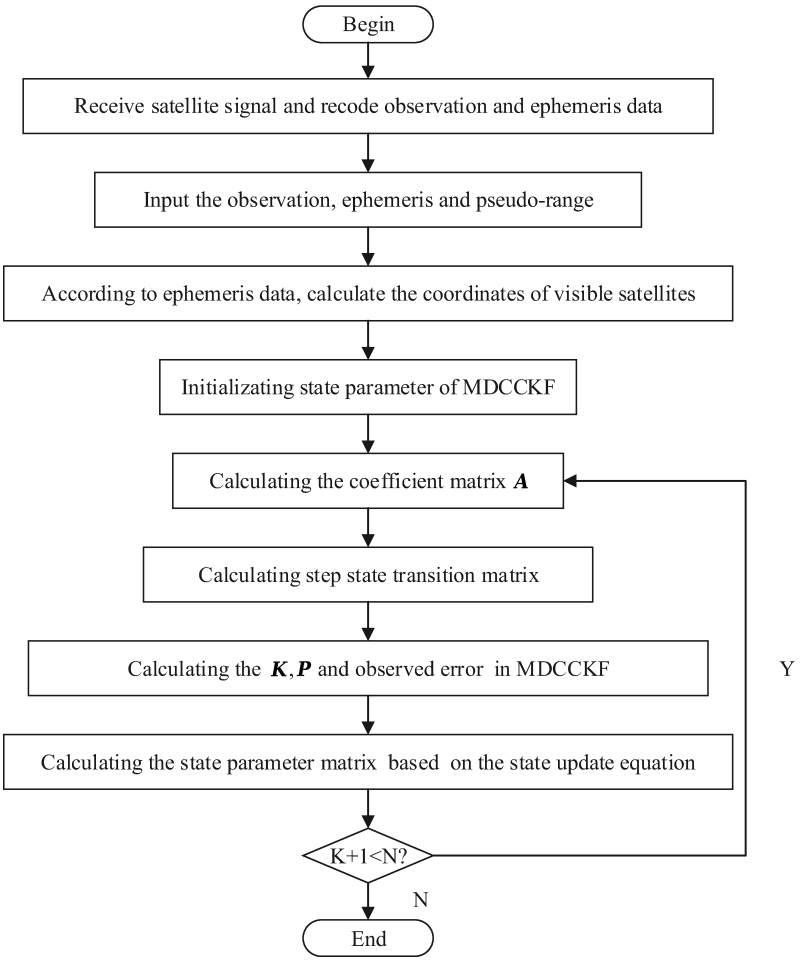

Fig. 1. The flowchart of MDCCKF positioning algorithm

4. Numerical results and analyses

To verify the validity of the MDCCKF positioning algorithm, this paper collects BDS's signal to solve the positioning result, and then analyzes the results by comparing with the original KF algorithm in terms of accuracy and robustness.

4.1. Data pre-processing

OEM6®Family Firmware which is produced by NovAtel Company is used to collect the satellite data. The state information of satellites can be obtained using the host computer software. By connecting the antenna, the OEM6®firmware can receive the ephemeris parameters of the satellites.

Fig. 2 shows the work of the BDS data collection under several different circumstances, including the vast environment, as well as many trees and the high-rise environment. As it is shown in Fig. 3, the current state information of satellites is given intuitively. The acquired satellite ephemeris information converted into RINEX format can be used for positioning solution. With the ephemeris parameters, the coordinates of the visible satellites can be obtained and used for positioning calculation.

(a)

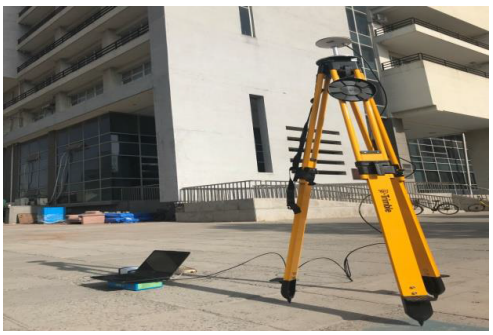

(b)

(c)

Fig. 2. Data collection under different experiments of BDS: vast environment (a); high-rise environment (b); lots of trees environment (c)

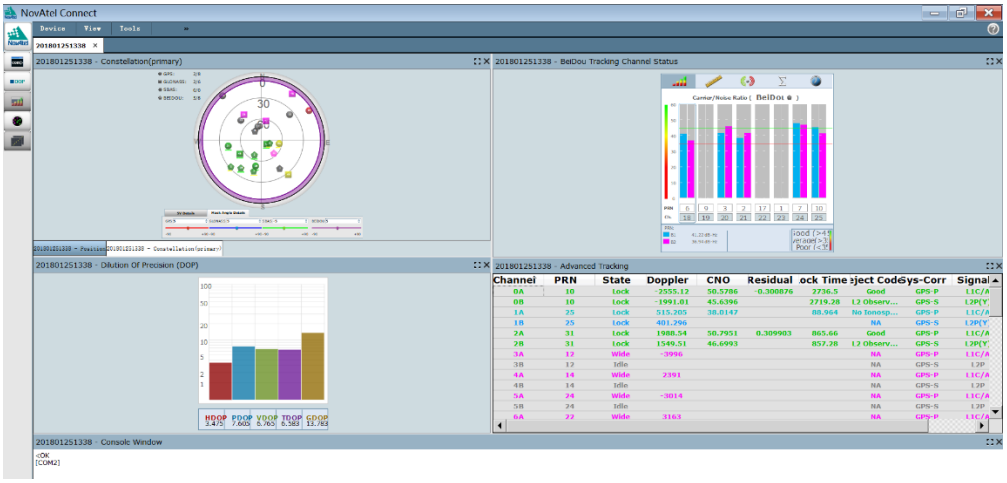

Fig. 3. Interface of BeiDou satellites states

To solve the coordinates of receivers, four or more satellite data should be required. We monitored the satellite status information within 6000 s as shown in Fig. 4. During the period of monitoring, the BeiDou satellites' conditions met the positioning requirements.

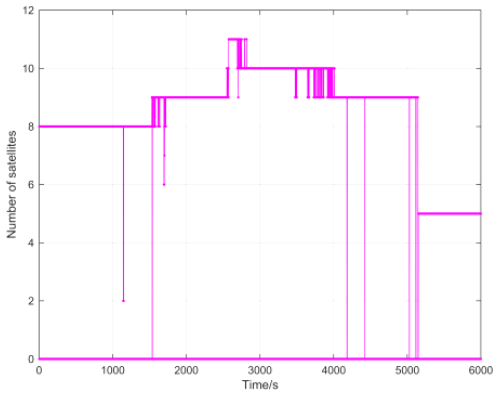

Fig. 4. The number of BeiDou satellites

Based on the information of satellite position and pseudo-range, the receiver can obtain coordinate of itself in the CGCS2000 coordinate system [30].

4.2. Parameter setting and positioning accuracy comparison

According to the above theoretical research, the performance of the MDCCKF algorithm proposed in this paper is evaluated according to real measured data, and the filtering effects of the MDCCKF and KF algorithms are compared and analyzed. In the background of non-Gaussian noise described by the ASD, it's verified that the MDCCKF algorithm has better performance than the traditional KF algorithm. The paper gives the noise distribution firstly, and then verifies

the effect of different dispersion coefficient γ and pulse index α on the positioning error result respectively.

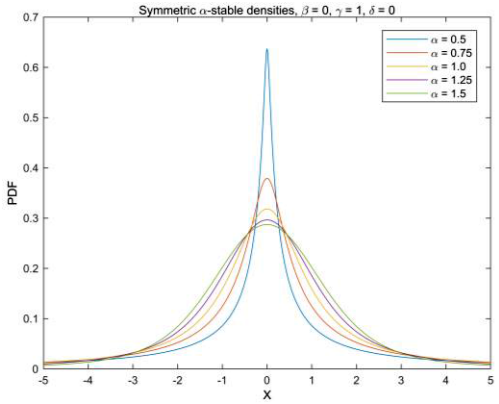

Fig. 5. The PDF of ASD noise

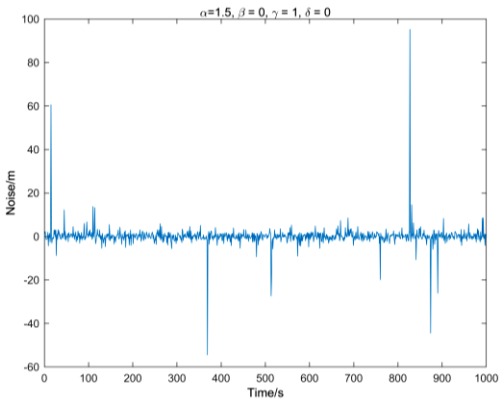

Fig. 6. The distribution of ASD noise

Due to the multipath effect and object obstruction, the observed noise of the BDS often does not obey the Gaussian distribution, and a small amount of large abnormal points will be generated. Therefore, the noise in this paper adopts the non-Gaussian model with alpha-stable distribution. Fig. 5 shows the PDF of standard $S\alpha S$ distribution at different α value correspondingly. Among them, according to the PDF of $\alpha = 1.5$ chosen randomly, Fig. 6 shows the noise model of $S\alpha S$ using 1000 noise samples. It can be seen that there are many abnormal noise points so that the observed noise often has a strong pulse. What's more, the smaller α is, the stronger the pulse is; and the larger α is, the closer it is to the Gaussian distribution.

Based on the real measured satellite data and the introduction of the ASD, the positioning accuracy of the BDS with the two algorithms can be obtained respectively. According to characteristic function (20), the ASD is determined by four parameters α, β, γ, δ. β is the symmetric coefficient; δ is the position parameter. When $\beta = \delta = 0$, the PDF of the ASD is symmetrical about Y axis, subjected to the $S\alpha S$ distribution. On the basis of the $S\alpha S$distribution the relationship between positioning accuracy and parameters α, γ is studied. γ is the dispersion coefficient of the ASD which is similar to the variance of the Gaussian distribution. Fig. 7 shows the curve of positioning accuracy with varying γ when $\alpha = 1$. It can be seen that the MDCCKF has a high accuracy when $\gamma \in [0.5, 1]$.

In the Gaussian noise environment, γ is equivalent to $2\sigma^2$. When $\gamma = 2\sigma^2 = 1$, the positioning errors of the KF and the MDCCKF algorithms with the changes of α are shown in Fig. 8. When $\alpha < 1$, the ASD has too many pulses so that it cannot be used as a statistical model of signal processing. Moreover, when $p < \alpha < 1$, the error function will no longer be a convex function so that the convergence algorithm will be very complicated. Therefore, the value range of α in this paper is $[1, 2]$. The comparison between the two algorithms shows that the MDCCKF algorithm has higher accuracy obviously, especially when $\alpha \in [1,\ 1.5]$.

It can be seen that the differences of positioning accuracy in Fig. 8 are apparent, when $\alpha \in [1,\ 1.5]$, while the positioning accuracy of two algorithms does not have much difference

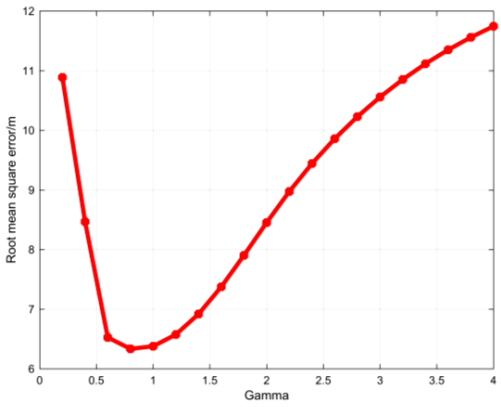

Fig. 7. The positioning error of different

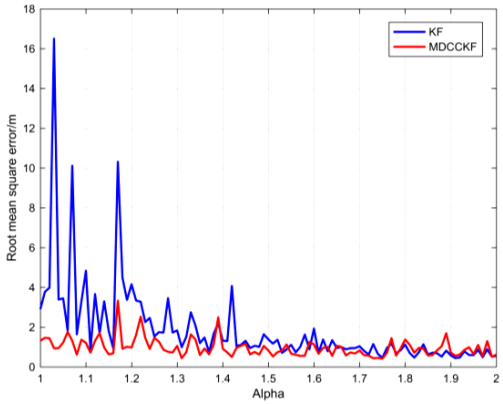

Fig. 8. The positioning error of different

when $\alpha \in [1.5, 2]$. Therefore, upon studying dynamic filtering within a certain time range, the two intervals should be considered separately. The median value of these two intervals is adopted in this paper, namely $\alpha = 1.25$ and $\alpha = 1.75$, to compare the positioning accuracy of the KF and MDCCKF algorithms. In order to ensure a reasonable positioning accuracy and be consistent with previous experiments, the dispersion coefficient and variance are still set as $\gamma = 2\sigma^2 = 1$.

Fig. 9 illustrates the curve of positioning errors within 300 s when $\alpha = 1.25$. It can be concluded that the MDCCKF algorithm has higher accuracy and enters a steady state faster compared with the original KF algorithm. To better show the error distribution, Fig. 10 illustrates the PDF of the positioning errors of the two algorithms. Most errors of the MDCCKF algorithm concentrate around 0.6 m while the error distribution of the KF algorithm is more dispersed and has a longer tail. It is clearly demonstrated that the MDCCKF algorithm has a concentrated distribution of the positioning error.

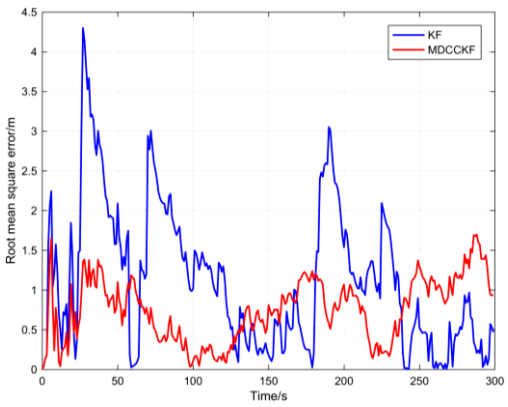

Fig. 9. The position error of BDS ($\alpha = 1.25$)

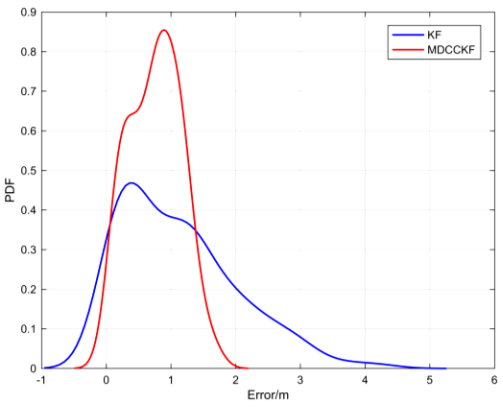

Fig. 10. The PDF of positioning error ($\alpha = 1.25$)

Fig. 11 shows the curve of the positioning error within 300 s when $\alpha = 1.75$. According to the characteristics of the ASD, the noise is closer to the Gaussian distribution compared with $\alpha = 1.25$. It can be seen from Fig. 11 that there is a significant reduction of the positioning error in both algorithms, but the error of the MDCCKF algorithm is still much smaller than that of the KF algorithm. Moreover, the curve of the MDCCKF algorithm maintains better stability and Fig. 12 shows that most errors of the MDCCKF algorithm concentrate around 0.4 m while that of the KF algorithm is about 1m. Similar to Fig. 10, Fig. 12 still shows that the KF algorithm has a longer tail, which means there's a larger positioning error. Therefore, the MDCCKF algorithm can effectively reduce the BDS's positioning error and maintain better stability.

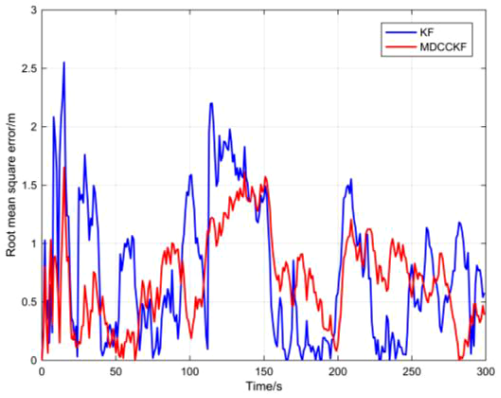

Fig. 11. The position error of BDS ($\alpha = 1.75$)

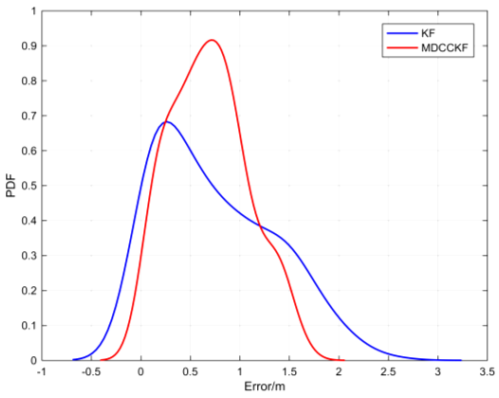

Fig. 12. The PDF of positioning error ($\alpha = 1.75$)

Through the real data collection and experimental research, it is proved that the MDCCKF algorithm can effectively eliminate the abnormal points in the signal and improve the accuracy of the positioning algorithm. At the same time, the MDCCKF algorithm can reach a steady state faster. And after reaching a stable state, the MDCCKF algorithm has better estimation performance and good robustness.

5. Conclusion

To solve the problem that the original KF algorithm can not deal with non-Gaussian noise effectively, this paper presents a MDCCKF algorithm. Based on the MDCC principle, the MDCCKF algorithm can remove the influence of non-Gaussian noise on the input signal, thereby improving the BDS's positioning accuracy. The research results show the MDCCKF algorithm has higher accuracy in the non-Gaussian noise environment, which ensures the stability of the positioning algorithm. The results give us an insightful future to improve the competitiveness of the system. Even in abnormal circumstances, the BDS can also ensure the accuracy of positioning results. In the future, after full verification by the BDS, the MDCCKF algorithm will also be able to help improve the GNSS's performance and even other positioning areas.

www.czasopisma.pan.pl PAN POLSKA AKADEMIA NAUK www.journals.pan.pl

Acknowledgements

We gratefully acknowledge the anonymous reviewers who read drafts and made many helpful suggestions. This work is supported by the National Natural Science Foundation of China under Grant No. 61701020, the University of Science and Technology Beijing Project under Grant No. 04130017, the Fundamental Research Funds for the Central Universities under Grant No. FRF-BD-17-015A, the Foundation of Beijing Engineering and Technology Center for Convergence Networks and Ubiquitous Services and Beijing Key Laboratory of Knowledge Engineering for Materials Science.

References

[1] Zhongming Z., Linong L., Xiaona Y., *Recent progresses on Beidou/COMPASS and other Global Navigation Satellite Systems (GNSS)-1*, Advances in Space Research, vol. 51, no. 6 (2013).

[2] Zhou Y., Chen X., Mao X., *A double-frequency combined positioning algorithm of BeiDou navigation satellite system*, 14th International Computer Conference on Wavelet Active Media Technology and Information Processing (ICCWAMTIP), Chengdu, China, pp. 9–14 (2017).

[3] Montenbruck O., Hauschild A., Steigenberger P., *Initial assessment of the COMPASS/BeiDou-2 regional navigation satellite system*, GPS solutions, vol. 17, no. 2, pp. 211–222 (2013).

[4] Jiang W., Xi R., Chen H., *Accuracy analysis of continuous deformation monitoring using BeiDou navigation satellite system at middle and high latitudes in China*, Advances in Space Research, vol. 59, no. 3, pp. 843–857 (2017).

[5] Li D., He G., Wu C., *Algorithm for autonomous navigation of mobile robot measurements based on Beidou/laser radar*, 2017 2nd Asia-Pacific Conference on Intelligent Robot Systems (ACIRS), IEEE,, Wuhan, China, pp. 305–309 (2017).

[6] Han Z., Liu J., Li R., *A modified differential coherent bit synchronization algorithm for BeiDou weak signals with large frequency deviation*, Sensors, vol. 17, no. 7, p. 1568 (2017).

[7] Wang X., Du J., Li W., *An improved high-sensitivity acquisition algorithm for BDS B2 signal*, China Satellite Navigation Conference, Shanghai, China, pp. 57–68 (2017).

[8] Dubovik O., Herman M., Holdak A., *Statistically optimized inversion algorithm for enhanced retrieval of aerosol properties from spectral multi-angle polarimetric satellite observations*, Atmospheric Measurement Techniques, vol. 4, no. 5, p. 975 (2011).

[9] Guo J., Zhang X., *Algorithm of GNSS positioning based on Doppler shift in incomplete condition of insufficient available satellites*, AOPC 2017: Space Optics and Earth Imaging and Space Navigation. International Society for Optics and Photonics, Beijing, China, p. 104630F (2017).

[10] Huang J., Tan H.S., *A low-order DGPS-based vehicle positioning system under urban environment*, IEEE/ASME Transactions on mechatronics, vol. 11, no. 5, pp. 567–575 (2006).

[11] Soubielle J., Fijalkow I., Duvaut P., *GPS positioning in a multipath environment*, IEEE Transactions on Signal Processing, vol. 50, no. 1, pp. 141–150 (2002).

[12] Viandier N., Nahimana D.F., Marais J., *GNSS performance enhancement in urban environment based on pseudo-range error model*, Position, Location and Navigation Symposium, California, United States, pp. 377–382 (2008).

[13] He F., Zhou S.S., Hu X.G., *Satellite-station time synchronization information based real-time orbit error monitoring and correction of navigation satellite in Beidou System*, Science China Physics, Mechanics & Astronomy, vol. 57, no. 7, pp. 1395–1403 (2014).

[14] Li M., Qu L., Zhao Q., *Precise point positioning with the BeiDou navigation satellite system*, Sensors, vol. 14, no. 1, pp. 927–943 (2014).

www.czasopisma.pan.pl PAN POLSKA AKADEMIA NAUK www.journals.pan.pl

[15] Takeuchi I., Bengio Y., Kanamori T., *Robust regression with asymmetric heavy-tail noise distributions*, Neural Computation, vol. 14, no. 10, pp. 2469–2496 (2002).

[16] Zechner C., Seelig G., Rullan M., *Molecular circuits for dynamic noise filtering*, Proceedings of the National Academy of Sciences of the United States of America, vol. 113, no. 17, pp. 4729–4734 (2016).

[17] Choi H.D., Ahn C.K., Lim M.T., *Time-domain filtering for estimation of linear systems with colored noises using recent finite measurements*, Measurement, vol. 46, no. 8, pp. 2792–2797 (2013).

[18] Plataniotis K.N., Androutsos D., Venetsanopoulos A.N., *Nonlinear filtering of non-Gaussian noise*, Journal of Intelligent and Robotic Systems, vol. 19, no. 2, pp. 207–231 (1997).

[19] Nolan J.P., *Fitting data and assessing goodness-of-fit with stable distributions*, PhD Thesis, Department of Mathematics and Statistics, American University, Washington DC (1999).

[20] Shao M., Nikias C.L., *Signal processing with fractional lower order moments: stable processes and their applications*, Proceedings of the IEEE, vol. 81, no. 7, pp. 986–1010 (1993).

[21] Magill D., *Optimal adaptive estimation of sampled stochastic processes*, IEEE Transactions on Automatic Control, vol. 10, no. 4, pp. 434–439 (1965).

[22] Izanloo R., Fakoorian S.A., Yazdi H.S., *Kalman filtering based on the maximum correntropy criterion in the presence of non-Gaussian noise*, 2016 Annual Conference on Information Science and Systems (CISS), IEEE, New Jersey, USA, pp. 500–505 (2016).

[23] Kemp F., *An introduction to sequential Monte Carlo methods*, Journal of the Royal Statistical Society: Series D (The Statistician), vol. 52, no. 4, pp. 694–695 (2003).

[24] Li D., Xu L., Li X., *Influence of UTC parameters generating method on BDS positioning accuracy*, Frequency and Time Forum and IEEE International Frequency Control Symposium (EFTF/IFC), Paderborn, Germany, pp. 699–702 (2017).

[25] Kang C., *A differential dynamic positioning algorithm based on GPS/Beidou*, Procedia engineering, vol. 137, pp. 590–598 (2016).

[26] Julier S.J., Uhlmann J.K., *Unscented filtering and nonlinear estimation*, Proceedings of the IEEE, vol. 92, no. 3, pp. 401–422 (2004).

[27] Chen B., Liu X., Zhao H., *Maximum correntropy Kalman filter*, Automatica, vol. 76, pp. 70–77 (2017).

[28] Liu W., Zhang H., Wang Z., *State estimation for discrete-time Markov jump linear systems based on orthogonal projective theorem*, International Journal of Control, Automation and Systems, vol. 10, no. 5, pp. 1049–1054 (2012).

[29] Lewis F.L., *Optimal estimation: with an introduction to stochastic control theory*, CRC Press (1986).

[30] Peng S., Zhao D., Huang Z., *Research and implementation of BDS/GPS coarse time navigation algorithm*, China Satellite Navigation Conference (CSNC), Changsha, China, pp. 227–240 (2016).